

Photonic Integrated Circuits using Crystal Optics (PICCO)

An overview

Thomas F Krauss^{1,*}, Rab Wilson¹, Roel Baets², Wim Bogaerts², Martin Kristensen³, Peter I Borel³, Lars H Frandsen³, Morten Thorhauge³, Bjarne Tromborg³, Andrej Lavrinenko³, Richard M De La Rue⁴, Harold Chong⁴, Luciano Socci⁵, Michele Midrio⁶, Stefano Boscolo⁶ and Dominic Gallagher⁷

¹University of St. Andrews, School of Physics and Astronomy, St. Andrews, UK.

²Ghent University - IMEC, Dept. of Information Technology (INTEC), Ghent, Belgium.

³Technical University of Denmark, Research Centre COM, Lyngby, Denmark.

⁴University of Glasgow, Dept. of Electronics & Electrical Engineering, Glasgow, UK.

⁵Pirelli Labs S.p.A, Advanced Photonics Research, Milan, Italy.

⁶University of Udine, Dept. of Electrical & Mechanical Engineering, Udine, Italy.

⁷Photon Design Europe Ltd. Oxford, UK.

* tfk@st-andrews.ac.uk

PICCO has demonstrated low loss, ultracompact photonic components based on wavelength-scale high contrast photonic microstructures and underpinned their design by sophisticated CAD tools. PICCO has also demonstrated device-fabrication via industrially viable deep UV lithography.

Introduction

Photonic crystals (PhCs) provide a fascinating platform for a new generation of integrated optical devices and components. Circuits of similar integration density as hitherto only known from electronic VLSI can be envisaged, finally bringing the dream of true photonic integration to fruition. What sets photonic crystals apart from conventional integrated optical circuits is their ability to interact with light on a wavelength scale, thus allowing the creation of devices, components and circuits that are several orders of magnitude smaller than currently possible. Apart from miniaturisation, a key property of photonic crystal components is their "designer dispersion", i.e. their ability to implement desired dispersion characteristics into the circuit. Functionalities include optical delay lines ("slow light"), optical pulse compression/dilation and wavelength splitters. In order to realise these functions, we need to understand the fundamental properties of photonic crystals and be able to fully master the technology of making them. Another key aspect is the understanding of the origin of propagation losses and their reduction to acceptable levels. While competitive values in terms of "loss per device" have now been demonstrated, the full potential of photonic crystal circuits will only be realised once many components can be cascaded together in complex circuits.

CAD tools

The ONYX-2 code [1], used for 3D-FDTD calculations, has been improved by implementing perfectly matched layers (PML) as absorbing boundaries, thereby effectively truncating the computational space in the program. The calculated 3D-FDTD spectra for PhC waveguide components are found to be in excellent agreement with experimentally observed spectra; the positions of dips and peaks in the spectra are typically predicted with an accuracy of 1-2% for SOI based components [2], and the actual measured propagation losses are also predicted correctly (fig. 2b).

Fabrication

E-beam lithography is the main lithographic workhorse of the consortium and is used extensively at Glasgow, also at COM and St. Andrews. It is a serial process, however, and thereby presents inherent limitations for high-volume mass-manufacture, so it is worthwhile to explore other routes to generating photonic crystal patterns. Classical photolithography, which is used for the current generation of planar lightwave circuits, lacks the resolution to fabricate these submicron structures with sufficient precision. Extending photolithography into the deep UV, however, where excimer lasers are used as light sources, changes the picture. With illumination wavelengths of 248 nm, moving on to 193 nm and eventually 157 nm, as well as projection optics with exceedingly high numerical apertures (nA), DUV lithography offers both the resolution and speed required for the high volume mass-manufacture of photonic circuits. Recent results obtained using 8" SOI wafers are very promising and highlight the viability of the process [3].

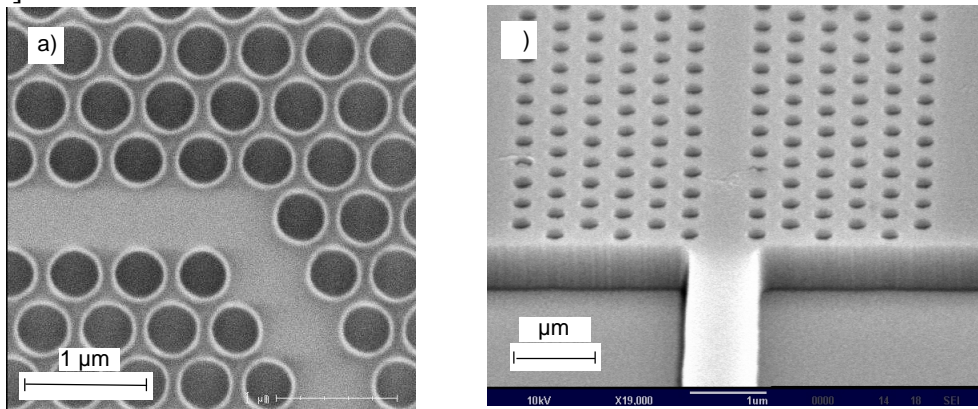


Fig. 1. SEM micrographs of photonic crystal waveguide patterns generated by DUV lithography. The period in both cases is 500 nm and the hole diameter is a) 380 nm and b) 230 nm.

Straight waveguides

Transmission properties of straight PhC waveguides have been investigated in the silicon-on-insulator (SOI) system. In the experiment, seven straight waveguides of type W1 (single line of missing holes) of lengths 10-150 μm were fabricated using e-beam lithography and reactive ion etching [4]. The holes were arranged in a triangular lattice with a period of $a=428$ nm (fig. 2a). 3D-FDTD calculations of transmission spectra for four straight PhCWs of lengths 29-59 μm were also performed. The measured and calculated propagation losses for TM polarised light are displayed in Fig. 2(b). The losses are

extracted by calculating the slope of the measured transmission as function of waveguide length. Good agreement is seen between experiment and simulation. Especially noteworthy is the 200 nm bandwidth with propagation losses around $9 \pm 5 \text{ dB/mm}$ for the TM polarisation. It is noted that even lower propagation losses, less than 4 dB/mm , have previously been observed in a narrower wavelength range [4].

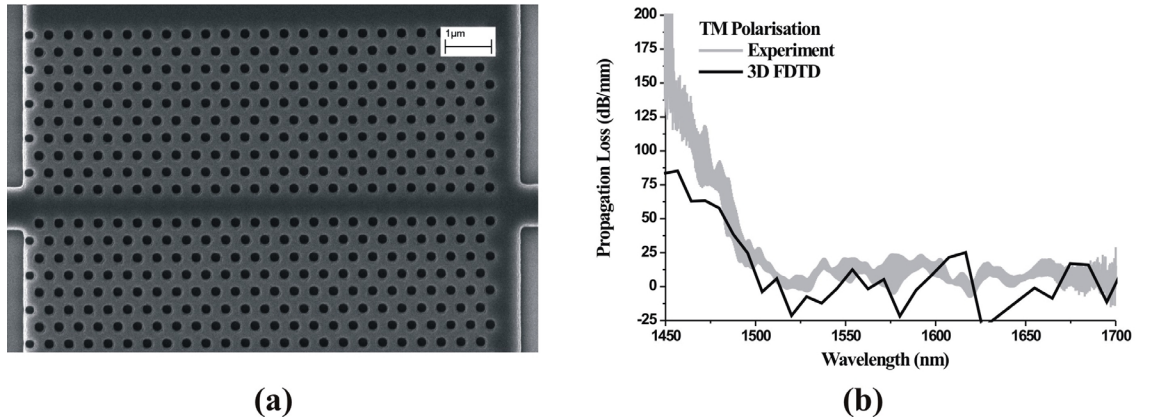


Fig. 2. (a) SEM micrograph of a straight PhC waveguide. (b) Measured and calculated propagation losses for TM polarised light in straight PhC W1 waveguides.

Y-junctions

While straight waveguides and bends have now been studied extensively, the very important problem of junctions that is essential for the operation of more complex circuits has only recently received attention [5-7].

Photonic crystals offer a real advantage in this case, as they make it possible, in principle, to construct 60° or even 90° bends at junctions, unlike in conventional integrated optics, where splitting angles are restricted to values around 2° . Let us consider the problem in more detail. If we join three W1 waveguides together, the 60° bend (or 120° split) is the most natural configuration in a triangular lattice. As light enters the junction, it experiences an optical volume that is slightly larger than that of the constituent waveguides, so the mode expands laterally. This mode expansion is analogous to that in a multi-mode interference (MMI) coupler and leads to the excitation of higher-order modes at the output port. These higher order modes typically cannot propagate and most of the light that enters the junction is reflected. This issue can be addressed by placing a smaller hole at the centre of the junction. The optical volume is then reduced, the mode cannot expand and the excitation of higher order modes is suppressed. As a result, efficient transmission over a wide bandwidth is observed [6].

This effect has also been observed experimentally. We used the configuration shown in figure 3a) and placed two smaller holes of increasing size at the centre of the junction in order to achieve a graded transition. The results are very encouraging, with a good balance between the two ports and a total transmission around 80% being observed (fig. 3 b,c).

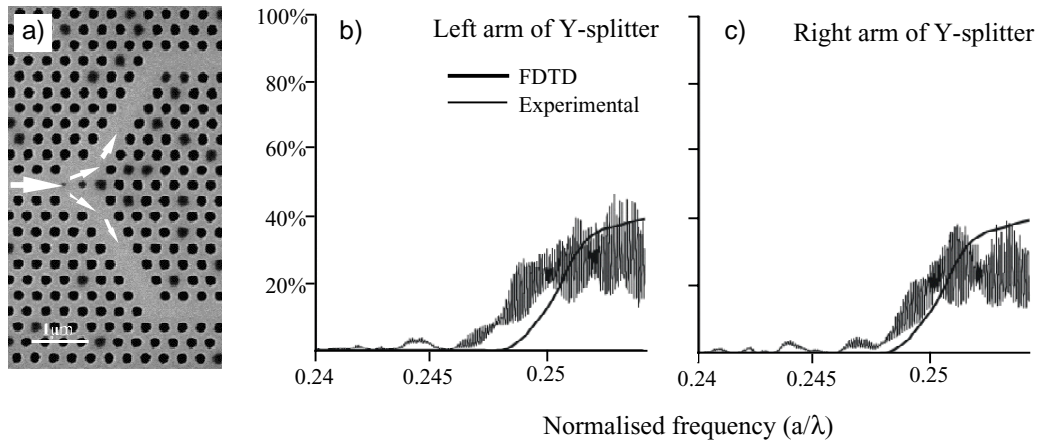


Fig. 3. SEM Micrograph and performance of a Y-junction with additional holes at the centre to avoid mode expansion. The vertical scale in b), c) represents transmission relative to a W1 waveguide. The oscillations in the experimental curves are due to Fabry-Perot resonances between the cleaved facets with superimposed resonances arising from reflections at the junction. The fact that the 2D FDTD agrees well with the 3D experiment indicates low out-of plane losses. The total transmission is between 70-80% over a relatively broad spectral range (30-40 nm @ 1300 nm). The bandwidth is limited by the bend rather than the junction.

Two of these Y-junctions mounted back-to-back constitute a Mach-Zehnder interferometer, which has also been operated successfully (passive, no tuning) with 28% transmission observed relative to a W1 waveguide. The design of the interferometer is extremely compact, with overall dimensions of the order of $10 \times 10 \text{ m}^2$.

Cavities

One of the functions obtainable from photonic crystal structures is wavelength division multiplexing, due to the strongly wavelength selective nature of cavities within a photonic crystal environment. Such properties have been demonstrated, e.g., by S. Fan *et al.*, [8] and S. Noda *et al.*, [9]. Cavities formed by in-filling one or more holes in a 2D photonic crystal have already shown high quality factors [10-12]. We have fabricated, in an SOI guide layer, such a cavity immediately adjacent to a channel waveguide and used a smaller diameter hole between cavity and waveguide to increase coupling. The Q of the cavity can be controlled by changing the hole diameter (and mode volume) and by using hole trimming inside the cavity.

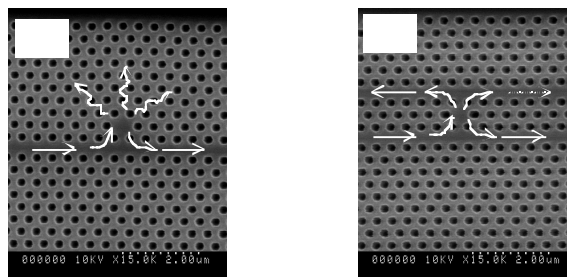


Fig 4. SEM micrographs of the single hole cavity with, (a) one channel waveguide giving drop function and (b) two channel waveguide providing add-drop function.

Cavities have also been fabricated for direct determination of the Q. Figure 3 (b) shows a single hole cavity with two channel waveguides where efficient adding or dropping of the resonant wavelength is expected from the decay rate of the resonance.

Circuits

While it is important to study individual devices, one of the ultimate aims of photonic crystal research is to realise more complex circuits. To this end, we have developed an analytical approach that allows us to engineer a complex circuit by borrowing simple concepts of propagation in transmission lines. Indeed, a photonic crystal waveguide may be seen as an equivalent transmission line that conveys equivalent currents and voltages among different loads. The loads may be formed by microcavities, junctions, bends, or even by an open waveguide that terminates into air, and they are all characterized by the fact that backreflections appear as soon as a guided field impinges on them. Once equivalent impedances are suitably defined for the photonic crystal waveguide and the loads, the behaviour of the circuit may be analytically described by looking at it as a connection of lumped elements, and use can be made of quantities that engineers have known for long time: the standing wave ratio, the partially standing waves the reflection coefficient, etc.

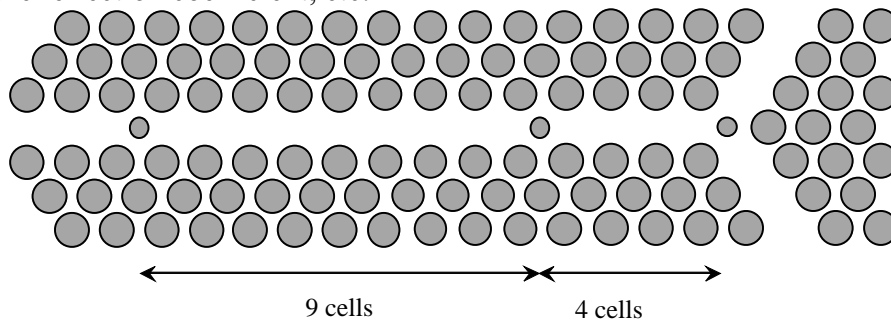


Fig 5. A Y-junction including tuning holes (double-stub tuner) to minimise reflections. A symmetric Y-junction has a maximum splitting ratio of 44.4% into the two output branches, whereas the Y-junction with tuner shown here achieves, theoretically, up to 49.3 % [6].

An example highlighting the potential of the approach is shown in Fig.5, where we optimize the transmission through the junction by *matching* its impedance to that of the incoming photonic crystal waveguide. This is done by designing an *equivalent double-stub network*, which is realized by introducing suitable defects in the input arm of the junction. The underlying physics is the following. When we insert a defect in the guide, and the guided mode impinges on it, higher order modes are excited in the vicinity of the defect itself. If these higher order modes are below cut-off, they can not propagate. In other words, they have an imaginary wave impedance, which gives rise to an unbalance between electric and magnetic stored energies, i.e. they form an equivalent lumped reactive element

Discussion and Conclusion

Several examples of miniaturised photonic crystal circuit elements have now been demonstrated, such as low-loss waveguides, Y-junctions and cavity waveguides. We are also beginning to understand how to combine these elements into more complex circuits using impedance matching techniques, and how to fabricate photonic crystal circuits on a larger scale using DUV lithography. While this makes a clear argument in favour of the photonic crystal approach, miniaturisation alone may not be sufficient to

ensure their major impact in integrated optics. Take WDM components as an example; the photonic crystal approach will only succeed if miniaturisation can be achieved with comparable or better performance than already offered by existing devices. State-of-the-art arrayed waveguide gratings (AWGs), for example, offer 50 GHz channel spacing with a channel accuracy of 2.5GHz and a crosstalk in excess of 30dB. These are benchmarks that are presently well out of reach of photonic crystal circuits. While it is clearly worthwhile to achieve similar performance with photonic crystals, we also need to look for applications that come more natural or offer solutions that cannot otherwise be achieved.

Such an application would be an amplifier with integrated dispersion control, or a detector with tunable dispersion compensation at the input side. Alternatively, the effective light-matter interaction in a modulator could be increased via slow wave structures, i.e. photonic crystal waveguides that operate in a low group velocity regime. This should allow modulators to be realised with effective electro-optic coefficients that scale with the reduction in group velocity and can therefore be much shorter.

Overall, while much progress has been made, the real killer application has yet to be developed.

References

1. A.J. Ward and J.B. Pendry, *Comp. Phys. Com.* **128**, 590-621 (2000).
2. P.I. Borel, M. Thorhauge, L.H. Frandsen, J. Cheng, M. Kampanis, M. Kristensen, A. Lavrinenko, Y. Zhuang and H.M.H. Chong, accepted for CLEO-Europe 03.
3. Bogaerts, W, Wiaux, V, Taillaert, D, Beckx, S, Luyssaert, B, Bienstman, P and Baets, R., *IEEE J. Select. Topic. Quantum Electron.* **8**, 928 (2002).
4. Arentoft, J, Sondergaard, T, Kristensen, M, Boltasseva, A, Thorhauge, M and Frandsen, L. 2002, *Electron. Lett.* **38**, 27 (2002).
5. Lin, SY, Chow, E, Bur, J, Johnson SG and Joannopoulos, JD, *Opt. Lett.* **27**, 1400 (2002).
6. Boscolo, S, Midrio, M and Krauss, TF, *Opt. Lett.* **27**, 1001 (2002).
7. Wilson, R, Karle, T and Krauss, TF, submitted for publication.
8. Fan, S, Villeneuve, P, and Joannopoulos, JD, *Phys. Rev. Lett.* **80**, 960, (1998).
9. Noda, S, Chutinan, A, and Imada, M, *Nature*, **407**, 608, (2000).
10. Smith, CJM, Krauss, T, Benisty, H, Rattier M, Weisbuch, C, Oesterle, U, Houdre, R, *J. Opt. Soc. Am. B*, **17**, 12, 2043, (2000).
11. Painter, O, Vuckovic, J, and Scherer, A, *J. Opt. Soc. Am. B*, **16**, 2, 275, (1999).
12. Scherer, A, Painter, O, Vukovic, J, Loncar, M, Yoshie, T, *IEEE Trans. Nano*, **1**, 1, 4, (2002).